Short Communication

Energy Levels of InGaAs/GaAs Quantum Dot Lasers with Different Sizes

E. Rajaei[*]**and M. A. Borji**

Department of Physics, Faculty of Science, University of Guilan, Rasht, I.R.Iran

(∗) Corresponding author: raf404@guilan.ac.ir

Abstract
In this paper, we have studied the strain, band-edge, and energy levels of cubic InGaAs quantum dots (QDs) surrounded by GaAs. It is shown that overall strain value is larger in InGaAs-GaAs interfaces, as well as in smaller QDs. Also, it is proved that conduction and valence band-edges and electron-hole levels are size dependent; larger QD sizes appeared to result in the lower recombination energies. Moreover, more number of energy levels separate from the continuum states of bulk GaAs and come down into the QD separate levels. In addition, we show that change of band gap and energy level by size is not linear, i.e., band gap and energy level in smaller QDs are more sensitive to QD size. Our results coincide with former similar researches.
Keywords : Band-edge, Engineering energy levels, QD laser, Quantum dot size, Strain PACS numbers: 73.63.Kv; 85.35.Be; 42.55.Px.

1. INRODUCTION

Semiconductor lasers have found many applications, and among many types of them, Quantum dot lasers have found a special place in new life due to their interesting characteristics arising from their discrete energy levels. Effects of various factors such as QD size (Baskoutas and Terzis, 2006; Pryor, 1998), percentage of constituent elements of the QD (Shi et al., 2011; Borji and Rajaei, 2016), substrate index (Povolotskyi et al., 2004; Rajaei and Borji, 2015b), strain (Pryor and Pistol, 2005; Shahraki and Esmaili, 2012), usage temperature (Chen and Xiao, 2007; Kumar et al., 2015; Narayanan and Peter, 2012; Rossetti et al., 2009; Borji and Rajaei, 2015a), wetting layer (WL), and distribution of QDs are shown to be important in the energy levels and performance of quantum dot lasers (Rajaei and Borji, 2015a; Borji and Rajaei, 2015b). Thus, finding the effect of these factors can be instructive in optimizing the laser performance. QD size effects are interesting and important, since it can change recombination energies and carrier relaxation and recombination times (Heitz et al., 1997).

Quantum dots and other dimensionally confined structures have been the focus of many researches due to their optical properties arising from the dimensional confinement of carriers (Markéta ZÍKOVÁ, 2012, Ma et al., 2013; Danesh Kaftroudi and Rajaei, 2010; Nedzinskas et al., 2012; Vafafard et al., 2013; Mortezapour et al., 2015). They have found many applications in semiconductor lasers and optical amplifiers (Bimberg et al., 2000; Gioannini, 2006; Danesh Kaftroudi and Rajaei, 2011; Asryan and Luryi, 2001). $In_x Ga_{1-x} As$/GaAs devices are now widely used in laser devices (Woolley et al., 1968; Nedzinskas et al., 2012; Hazdra et al., 2008; Fali et al., 2014; Yekta Kiya et al., 2012; Shafieenezhad et al., 2014); thus, a ubiquitous view of the energy states, band-edges, strain, and other

features, and their variation by QD size can be helpful.

Color of laser received from a QD laser is determined by the band gap width. In bulk semiconductors band gap is fixed. However, this situation changes in QDs, i.e., electrons will be sensitive to the nano-scale boundaries and adjust their energy which results in the change of laser color. In semiconductor hetero-structures which contain more than one material, energy states appear to be more complex than bulk samples due to the significant role of strain. Strain tensor depends on lattice mismatch, elastic properties of neighbor materials, and geometry of the QD (Trellakis et al., 2006). This research represents a quantum numerical study of the energy states, band structure, and strain tensor of $In_{0.2}Ga_{0.8}As$ QDs grown on GaAs substrate. This composition is previously used in some works; see for example (Kazi et al., 2001).

The rest of this paper is organized as follows: section II explains the numerical model; results and discussions are presented in section III; finally, we make a conclusion in section IV.

2. NUMERICAL MODEL

Having formulated the dot structure, band energies of a zinc-blende crystal is obtained next by Schrödinger equation:

$$\left(H_0 + H_k + H_{k.p} + H_{s.o.} + H'_{s.o.}\right)u_{nk}(r) = E_n(\mathbf{k})u_{nk}(r) \quad (1)$$

With $u_{nk}(r)$ as the periodic Bloch function and

$$H_0 = \frac{p^2}{2m_0} + V_0(r, \varepsilon_{ij}) \quad (2)$$

$$H_k = \frac{\hbar^2 k^2}{2m_0} \quad (3)$$

$$H_{k.p} = \frac{\hbar}{m_0} k \cdot p \quad (4)$$

$$H_{s.o.} = \frac{\hbar}{4m_0^2 c^2}\left(\sigma \times \nabla V_0(r, \varepsilon_{ij})\right) \cdot p \quad (5)$$

$$H'_{s.o.} = \frac{\hbar}{4m_0^2 c^2}\left(\sigma \times \nabla V_0(r, \varepsilon_{ij})\right) \cdot \hbar k \quad (6)$$

In these equations i, j stand for x, y, or z. σ is the Pauli spin matrix, $V_0(r, \varepsilon_{ij})$ is the periodic potential of the strained crystal, c

is the light velocity, and m_0 is the mass of electron. This equation can be solved by expansion of $V_0(r, \varepsilon_{ij})$ to first order in strain tensor ε_{ij} (Bahder, 1990). In the Cartesian system the solution is:

Table1. Parameters used in the model.

Parameter	GaAs	InAs
Band gap (0K)	1.424eV	0.417eV
lattice constant	0.565325 nm	0.60583 nm
Expansion coefficient of lattice constant	0.0000388	0.0000274
Effective electron mass (Γ)	0.067m$_o$	0.026m$_o$
Effective heavy hole mass	0.5m$_o$	0.41m$_o$
Nearest neighbor distance (300K)	0.2448 nm	0.262 nm
Elastic constants	$C_{11} = 122.1$ $C_{12} = 56.6$ $C_{44} = 60$	$C_{11} = 83.29$ $C_{12} = 45.26$ $C_{44} = 39.59$

$$E_n(\mathbf{k}) = E_n(\mathbf{0}) + \frac{\hbar^2 k_i k_j}{2}\left(\frac{1}{m_n^*}\right)_{i,j} \quad (7)$$

In which the tensor of the effective mass is defined as (Galeriu and B. S., 2005):

$$\left(\frac{1}{m_n^*}\right)_{i,j} =$$

$$\left(\frac{1}{m_0}\right)\delta_{i,j} + \frac{2}{m_0^2}\sum_{m \neq n}\frac{\langle n,0|p_i'|m,0\rangle\langle m,0|p_j'|n,0\rangle}{E_n(0) - E_m(0)}$$

$$\quad (8)$$

Parameters related used in this paper are given in Table 1 (Jang et al., 2003; Singh, 1993; Yu, 2010). Also, for $In_xGa_{1-x}As$ the parameters are calculated as follows:

Lattice constant at T=300K (Adachi, 1983):

$$a = (6.0583 - 0.405(1 - x)) \text{ Å} \quad (9)$$

Effective electron mass at 300K (T.P.Pearsall, 1982):

$$m_e = (0.023 + 0.037(1 - x) + 0.003(1 - x)^2)m_o \quad (10)$$

Effective hole mass at 300K (Schmidt, 1999):

$$m_h = (0.41 + 0.1(1 - x))m_o \quad (11)$$

Effective light-hole masses at 300K:

$$m_{lp} = (0.026 + 0.056(1 - x))m_o \qquad (12)$$

Effective split-off band hole-masses at 300K is $\sim 0.15\ m_o$.

In self-assembled QD growth, a WL with a few molecular layers is grown and millions of QDs are formed, each with a random shape and size. QDs are finally covered by a cap layer. Many shapes can be approximated for QDs, namely, cylindrical, cubic, lens shape, pyramidal (Qiu and Zhang, 2011), etc. For simplicity, the QDs are assumed here to be cubic and far enough to avoid any effects by neighbor QDs. The one-band effective mass approach is used in solving the Schrödinger equation, and the Poisson's equation was solved numerically in a self-consistent manner.

Figure 1 shows the cross-section of a $14 \times 14 \times 14 nm^3$ cubic $In_{0.2}Ga_{0.8}As$ QD surrounded by GaAs. The substrate and cap thickness are assumed here to be 20nm, and the wetting layer to be $0.5 nm$. This structure is grown on (001) substrate index. The growth-direction is along z-axis. The unstructured mesh is used for the system in which smaller meshes are included inside the QD region.
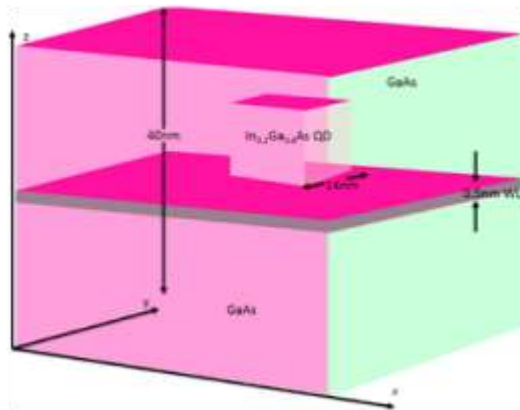

Figure1. *Profile of a cubic InGaAs QD of $14 nm \times 14 nm \times 14 nm$ on $20 nm$ thick GaAs substrate and $0.5 nm$ wetting layer. The meshes are seen in this figure.*

When changing QD size, all the sides change simultaneously and the cubic shape is fixed. Also, the cell volume changes since cap and substrate index are fixed.

3. RESULTS AND DISCUSSION

Strain is defined as the summation of all infinitesimal length increases relative to the instantaneous lengths ($\varepsilon_L = \sum \Delta L_t / L_t$). Thus, by taking into account length changes in all dimensions, one achieves a strain tensor

$$\varepsilon_{ij} = \frac{1}{2}\left(\frac{du_i}{dr_j} + \frac{du_j}{dr_i}\right) \qquad (13)$$

Where du_i is the length variation along direction i, and r_j is the length in direction j (Povolotskyi et al., 2004). Diagonal components concern with expansion along an axis (stretch), while off-diagonal ones denote rotation. In our case, the strain tensor is a diagonal matrix as follows:

$$\varepsilon = \begin{bmatrix} \varepsilon_{xx} & 0 & 0 \\ 0 & \varepsilon_{yy} & 0 \\ 0 & 0 & \varepsilon_{zz} \end{bmatrix} \qquad (14)$$

This tensor shows a biaxial in-plain strain defined as:

$$\varepsilon_{xx} = \varepsilon_{yy} = \varepsilon_{||} = \frac{a_{||} - a_{substrate}}{a_{substrate}} \qquad (15)$$

and a perpendicular uniaxial strain defined as (Peressi et al., 1998):

$$\varepsilon_{zz} = \varepsilon_{\perp} = -\frac{2C_{xy}}{C_{xx}}\varepsilon_{xx} = \frac{a_{\perp} - a_{substrate}}{a_{substrate}} \qquad (16)$$

Where C_{ij} are components of the matrix which interconnects stress σ to strain (i.e., $\sigma = C\varepsilon$) (Chuang and Chang, 1997).

Figure. 2 illustrates the two non-zero elements of the strain tensor, namely, ε_{xx} and ε_{zz} for two different QD sizes. As it is viewed, in both directions, strain tensor is subjected to change in interfaces. However, the near points appear to have different strains as well.

In Fig. 3 non-zero elements of strain tensor are plotted along z-direction and at the

middle cross-section of the structure. It can be argued that the existence of indium in one side of interfaces leads to a jump in the strain tensor meaning a stretch in GaAs and squeeze in InGaAs lattice constant.

Along z-direction, as it is observed, strain experienced in interfaces is different for different QD sizes; the value is more for smaller QDs which informs of more stretch exerting on few number of atoms existing in a smaller QD. To explain, we notice that lattice constant of GaAs and InAs is 0.565325nm and 0.60577nm respectively and it increases almost linearly by indium percentage (Qiu and Zhang, 2011).
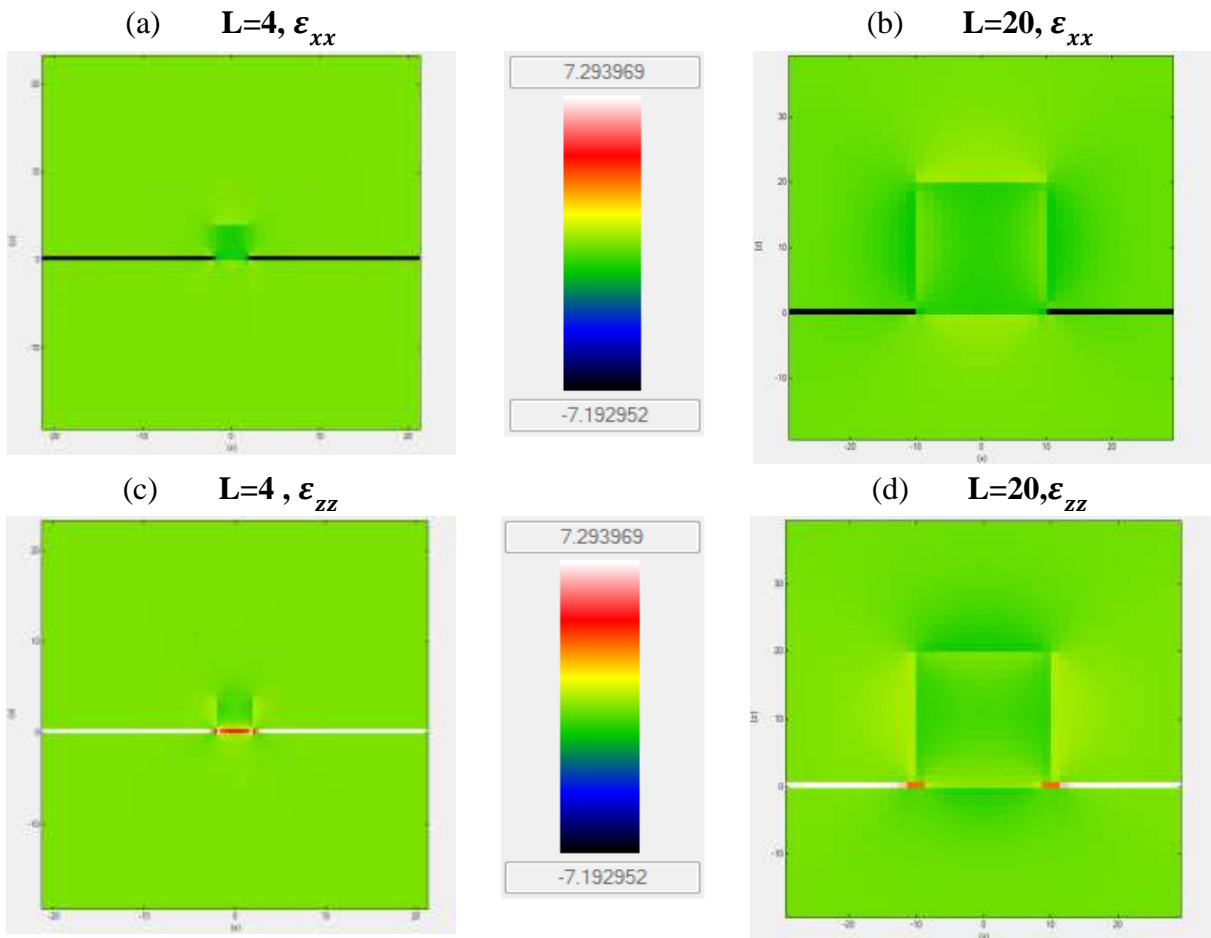
(a) **L=4, ε_{xx}**   (b) **L=20, ε_{xx}**

(c) **L=4 , ε_{zz}**   (d) **L=20,ε_{zz}**

Figure2. Strain tensor in different points of the device with L=4nm and L=20nm at T=295K
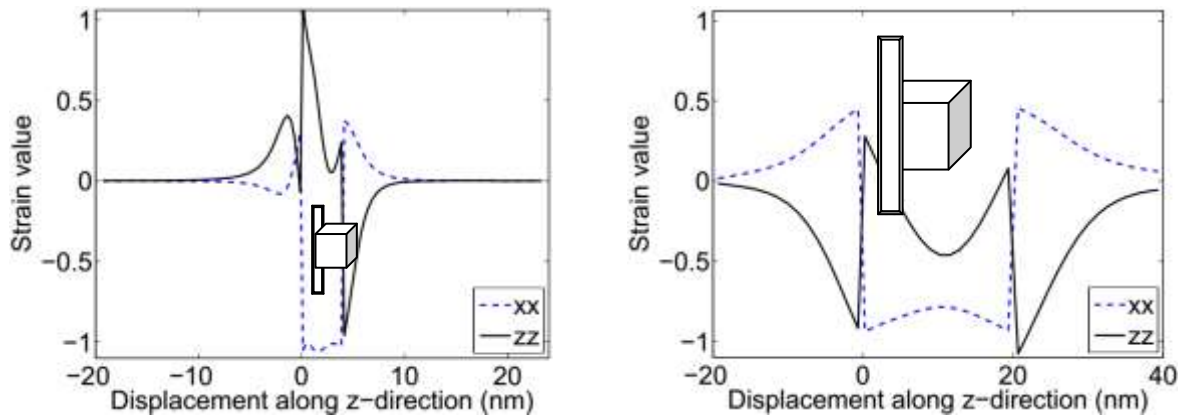

Figure3. Components of strain tensor at two different QD sizes.

         Rajaei and Borji

Strain is discussed in (Jiang and Singh, 1997) that is due to 7% mismatch of lattice constants of GaAs and InAs(Zhao et al., 2005). In fact, decreased QD size shortens the length along which atoms will match their lattice constant to the neighbor one. That is why they tolerate more tension and strain.

Figure. 4 depicts the Γ and Heavy-Hole (HH) band-edges of each point of QDs with different sizes on x-z plane in the middle cross-section of the structure. As it is observed, both conduction and valence band-edges have been fully subjected to change by size effect. Also, the cap layer band-edges have been subjected to change in the points close to the QD. Comparison of Fig. 4(a) with 4(c) or Fig. 4(b) with 4(d) shows that both electron- and hole-band-edges of the QD are sensitive to size.

In Figure. 5 conduction and valence band-edges in z-direction, and the first allowed energy state of electrons and holes are shown. As it is clear, QDs of side 4nm has no allowed energy state for electrons into the QD. But enlargement of QD side to 14nm leads to a lowered electronic state which lay into the QD. More increase of QD size results in the more separated energy levels laid into the QD. Moreover, the recombination energies have decreased by size. Other states are among continuous states of the GaAs. Since in a laser device the photons are results of the separate energies of the QD, the laser wavelength is expected to elongate in larger QDs. Some similar results can be seen in (Baskoutas and Terzis, 2006; Jiang and Singh, 1997; Pryor, 1998) in which the size dependence is confirmed. They show that increase of size in QDs lowers the band gap, raises the hole states and decrease the electronic states. Our results showed a consonance with their findings. In addition, energy gap for bulk InAs and GaAs are 0.36eV and 1.43eV respectively (Bratkovski and Kamins, 2010), but obviously, it changes here by size restriction.

In addition, change of conduction and valence band edges is shown in Fig. 6. Obviously QD size increase has enhanced the electronic band edge and decreased the heavy-hole band edge.
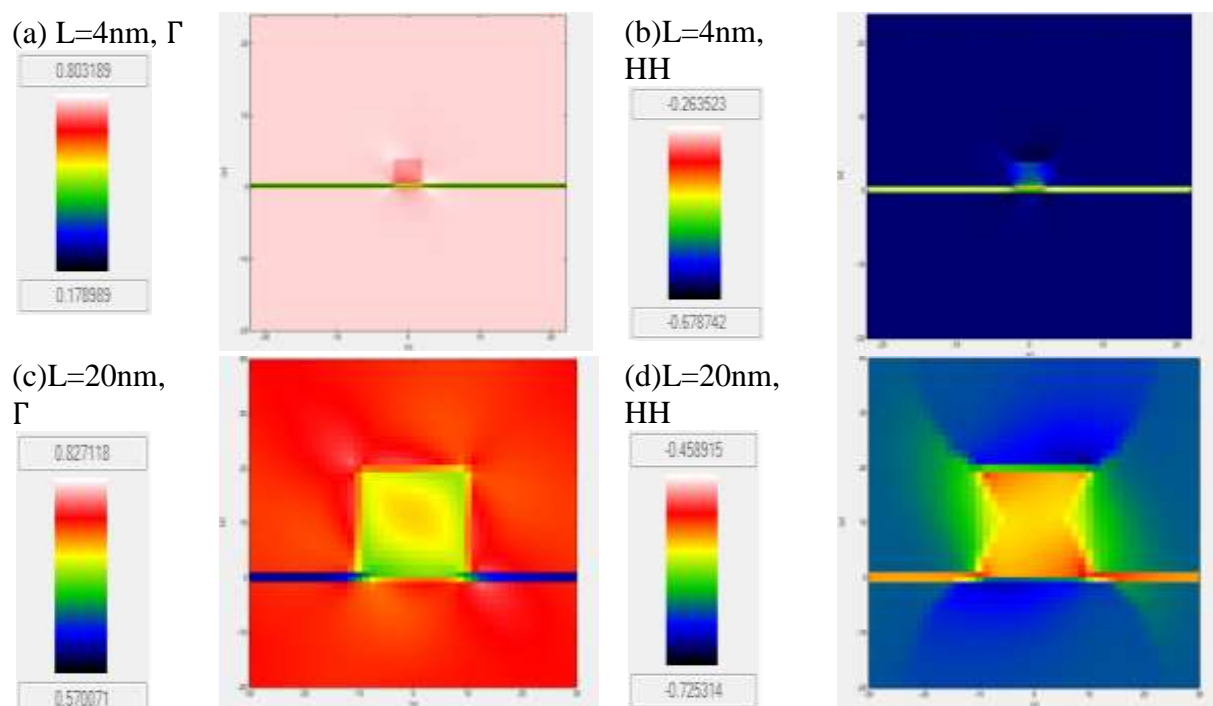
(a) L=4nm, Γ

(b)L=4nm, HH

(c)L=20nm, Γ

(d)L=20nm, HH

Figure4. *Valence and conduction band-edges in x-z plane in the cross-section of the QD. Note the numbers related to colors beside each figure.*
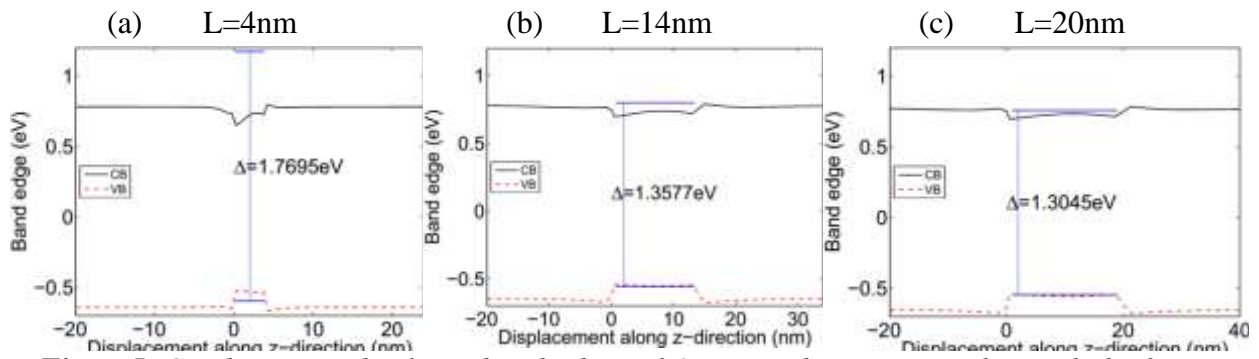
Figure5. *Conduction and valence band-edges of QDs in z-direction together with the first allowed energy states for electrons and holes at different sizes.*
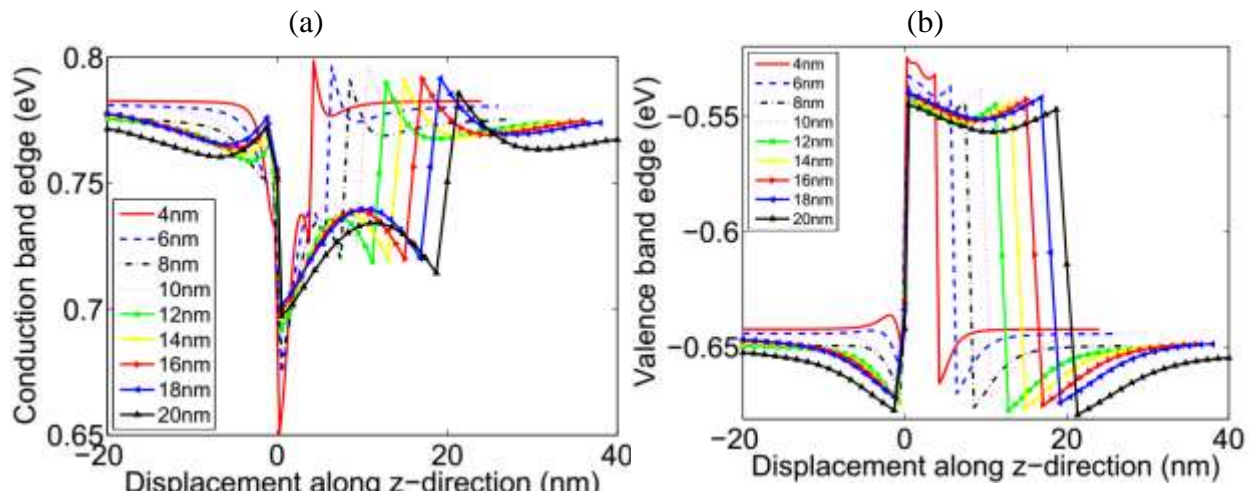

Figure6. *Conduction and valence band edges for various QD sizes*

Table2. *First five eigenvalues of electron and hole for different QD sizes*

QD Size (nm)	Level No	Electron energy (eV)	Hole energy (eV)	Recombination energy	Status
4	1	1.17	-0.59	1.76	**Among continuum states**
4	2	1.63	-0.65	2.28	**Among continuum states**
4	3	1.64	-0.65	2.30	**Among continuum states**
4	4	1.64	-0.66	2.30	**Among continuum states**
4	5	2.10	-0.71	2.81	**Among continuum states**
14	1	0.79	-0.55	1.35	**Into QD separate states**
14	2	0.86	-0.56	1.43	**Among continuum states**
14	3	0.86	-0.56	1.43	**Among continuum states**
14	4	0.87	-0.57	1.44	**Among continuum states**
14	5	0.94	-0.57	1.51	**Among continuum states**
20	1	0.75	-0.54	1.30	**Into QD separate states**
20	2	0.78	-0.54	1.33	**Into QD separate states**
20	3	0.78	-0.55	1.34	**Into QD separate states**
20	4	0.79	-0.55	1.35	**Into QD separate states**
20	5	0.82	-0.55	1.38	**Into QD separate states**

On the other hand, effect of size on the band edges is more for small QDs, but the results do not change much for QDs sizes of more than 8nm. This denotes that the effect of size on band edge is not linear.
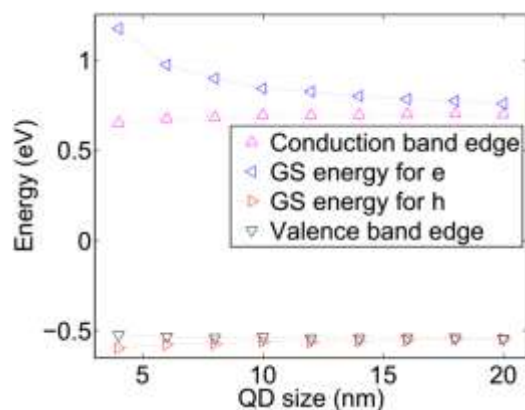

Figure7. *Energy gap of the ground state versus QD size*

Moreover, e-h energies as well as the valence and conduction bands are drawn in Fig. 7 as a function of QD size. The interesting result of this article is that QD size makes a nonlinear effect on recombination energy while band gap remains almost unchanged. Decreased recombination energy in larger QDs results in the elongated laser wavelength which should be regarded in fabrication of lasers. Note that in these figures hole states are almost insensitive to QD size and only electronic levels are subjected to change.

In addition, on Table 2 the first five eigenvalues of electron- and hole-states of different QD sizes are written. Clearly, size has changed the degeneracy of both electron and hole states as well as the recombination energies.

4. CONCLUSION

We studied the band structure and strain tensor of $In_{0.2}Ga_{0.8}As$ quantum dots grown on GaAs substrate by numerical solutions. It was shown that the total strain value is larger in the interfaces, and also in smaller QD sizes. The conduction and valence band-edges and electron-hole levels were found to be dependent on QD size as well; larger sizes resulted in the lower (higher) energy of electrons (holes). Thus, the recombination energies decreased in larger QDs. In addition, more number of energy levels separated from the continuum states of bulk GaAs and came down into the QD separate levels. Moreover, it was observed that degeneracy of levels was subjected to change by size variation. These results had a good consonance with Pryor et al results (Pryor and Pistol, 2005; Pryor, 1998).

REFERENCES

1. ADACHI, S. 1983. *J.Appl. Phys.,* vol. 54**,** 1844-1848.
2. ASRYAN, L. V. & LURYI, S. 2001. Tunneling-injection quantum-dot laser: ultrahigh temperature stability. *Quantum Electronics, IEEE Journal of,* 37**,** 905-910.
3. BAHDER, T. B. 1990. Eight-band k.p model of strained zinc-blende crystals. *Physical Review B,* 41**,** 11992-12001.
4. BASKOUTAS, S. & TERZIS, A. F. 2006. Size-dependent band gap of colloidal quantum dots. *Journal of Applied Physics,* 99**,** 013708.
5. BIMBERG, D., GRUNDMANN, M., HEINRICHSDORFF, F., LEDENTSOV, N. N., USTINOV, V. M., ZHUKOV, A. E., KOVSH, A. R., MAXIMOV, M. V., SHERNYAKOV, Y. M., VOLOVIK, B. V., TSATSUL'NIKOV, A. F., KOP'EV, P. S. & ALFEROV, Z. I. 2000. Quantum dot lasers: breakthrough in optoelectronics. *Thin Solid Films,* 367**,** 235-249.
6. BIRNER, S., ZIBOLD, T., ANDLAUER, T., KUBIS, T., SABATHIL, M., TRELLAKIS, A. & VOGL, P. 2007. nextnano: General Purpose 3-D Simulations. *Electron Devices, IEEE Transactions on,* 54**,** 2137-2142.

7. BORJI, M. A. & RAJAEI, E. 2015a. Effect of temperature on In_x Ga_(1-x) As/GaAs quantum dot lasing. *arXiv:1511.00996 [physics.comp-ph] (unpublished observations)*.
8. BORJI, M. A. & RAJAEI, E. 2015b. Influence of Indium-Percentage Variation on Dynamical Characteristics of InxGa1-xAs/GaAs(001) Quantum Dot Lasers. *arXiv:1511.00999 [physics.comp-ph] (unpublished observations)*.
9. BORJI, M. A. & RAJAEI, E. 2016. Energy Level Engineering in InxGa1-xAs/GaAs Quantum Dots Applicable to Quantum Dot-Lasers by Changing the Stoichiometric Percentage. *Journal of Nanoelectronics and Optoelectronics,* 11**,** 315-322.
10. BRATKOVSKI, A. & KAMINS, T. I. 2010. Nanowire-Based Light-Emitting Diodes and Light-Detection Devices With Nanocrystalline Outer Surface. Google Patents.
11. CHEN, S.-H. & XIAO, J.-L. 2007. Temperature Effect On Impurity-Bound Polaronic Energy Levels In A Parabolic Quantum Dot In Magnetic Fields. *International Journal of Modern Physics B,* 21**,** 5331-5337.
12. CHUANG, S. L. & CHANG, C. S. 1997. A band-structure model of strained quantum-well wurtzite semiconductors. *Semiconductor Science and Technology,* 12**,** 252.
13. DANESH KAFTROUDI, Z. & RAJAEI, E. 2010. Simulation And Optimization Of Optical Performance Of Inp-Based Longwavelength Vertical Cavity Surface Emitting Laser With Selectively Tunnel Junction Aperture. *Journal Of Theoretical And Applied Physics (Iranian Physical Journal),* 4**,** 12-20.
14. DANESH KAFTROUDI, Z. & RAJAEI, E. 2011. *Thermal simulation of InP-based 1.3 micrometer vertical cavity surface emitting laser with AsSb-based DBRs,* Amsterdam, PAYS-BAS, Elsevier.
15. FALI, A., RAJAEI, E. & KAFTROUDI, Z. 2014. Effects of the carrier relaxation lifetime and inhomogeneous broadening on the modulation response of InGaAs/GaAs self-assembled quantum-dot lasers. *Journal of the Korean Physical Society,* 64**,** 16-22.
16. GALERIU, C. & B. S., M. S., M. A. 2005. k. p theory of semiconductor nanostructures. *a dissertation submitted to the faculty of the Worcester polytechnic institute for degree of doctor of philosophy in physics***,** 11-13.
17. GIOANNINI, M. 2006. Analysis of the Optical Gain Characteristics of Semiconductor Quantum-Dash Materials Including the Band Structure Modifications Due to the Wetting Layer. *IEEE Journal of Quantum Electronics,* 42**,** 331-340.
18. HAZDRA, P., VOVES, J., OSWALD, J., KULDOVÁ, K., HOSPODKOVÁ, A., HULICIUS, E. & PANGRÁC, J. 2008. Optical characterisation of MOVPE grown vertically correlated InAs/GaAs quantum dots. *Microelectronics Journal,* 39**,** 1070-1074.
19. HEITZ, R., VEIT, M., LEDENTSOV, N. N., HOFFMANN, A., BIMBERG, D., USTINOV, V. M., KOP'EV, P. S. & ALFEROV, Z. I. 1997. Energy relaxation by multiphonon processes in InAs/GaAs quantum dots. *Physical Review B,* 56**,** 10435-10445.
20. JANG, Y. D., LEE, U. H., LEE, H., LEE, D., KIM, J. S., LEEM, J. Y. & NOH, S. K. 2003. Comparison of quantum nature in InAs/GaAs quantum dots. *Journal of the Korean Physical Society,* 42**,** 111-113.
21. JIANG, H. & SINGH, J. 1997. Conduction band spectra in self-assembled InAs/GaAs dots: A comparison of effective mass and an eight-band approach. *Applied Physics Letters,* 71**,** 3239-3241.
22. KAZI, Z. I., EGAWA, T., UMENO, M. & JIMBO, T. 2001. Growth of InxGa1−xAs quantum dots by metal–organic chemical vapor deposition on Si substrates and in GaAs-based lasers. *Journal of Applied Physics,* 90**,** 5463-5468.
23. KUMAR, D., NEGI, C. M. S. & KUMAR, J. 2015. Temperature Effect on Optical Gain of CdSe/ZnSe Quantum Dots. *In:* LAKSHMINARAYANAN, V. & BHATTACHARYA, I. (eds.) *Advances in Optical Science and Engineering.* Springer India.
24. MA, Y. J., ZHONG, Z., YANG, X. J., FAN, Y. L. & JIANG, Z. M. 2013. Factors influencing epitaxial growth of three-dimensional Ge quantum dot crystals on pit-patterned Si substrate. *Nanotechnology,* 24**,** 015304.
25. MARKÉTA ZÍKOVÁ, A. H. 2012. Simulation of Quantum States in InAs/GaAs Quantum Dots. *NANOCON* 23, 10.
26. MORTEZAPOUR, A., ABAD, M. G. G. & MAHMOUDI, M. 2015. Magneto-optical rotation in a GaAs quantum well waveguide. *Journal of the Optical Society of America B,* 32**,** 1338-1345.
27. NARAYANAN, M. & PETER, A. J. 2012. Pressure and Temperature Induced Non-Linear Optical Properties in a Narrow Band Gap Quantum Dot. *Quantum Matter,* 1**,** 53-58.
28. NEDZINSKAS, R., ČECHAVIČIUS, B., KAVALIAUSKAS, J., KARPUS, V., VALUŠIS, G., LI, L., KHANNA, S. P. & LINFIELD, E. H. 2012. Polarized photoreflectance and photoluminescence spectroscopy of InGaAs/GaAs quantum rods grown with As(2) and As(4) sources. *Nanoscale Research Letters,* 7**,** 609-609.
29. PERESSI, M., BINGGELI, N. & BALDERESCHI, A. 1998. Band engineering at interfaces: theory and numerical experiments. *Journal of Physics D: Applied Physics,* 31**,** 1273.

30. POVOLOTSKYI, M., DI CARLO, A., LUGLI, P., BIRNER, S. & VOGL, P. 2004. Tuning the piezoelectric fields in quantum dots: microscopic description of dots grown on (N11) surfaces. *Nanotechnology, IEEE Transactions on,* 3**,** 124-128.
31. PRYOR, C. 1998. Eight-band calculations of strained InAs/GaAs quantum dots compared with one-, four-, and six-band approximations. *Physical Review B,* 57**,** 7190-7195.
32. PRYOR, C. E. & PISTOL, M. E. 2005. Band-edge diagrams for strained III-V semiconductor quantum wells, wires, and dots. *Physical Review B,* 72**,** 205311.
33. QIU, D. & ZHANG, M. X. 2011. The preferred facet orientation of GaAs pyramids for high-quality InAs and InxGa1−xAs quantum dot growth. *Scripta Materialia,* 64**,** 681-684.
34. RAJAEI, E. & BORJI, M. A. 2015a. Impact of dot size on dynamical characteristics of InAs/GaAs quantum dot lasers. *arXiv:1511.01000 [physics.comp-ph (unpublished observations) Accepted to Journal of Nanoelectronics and Optoelectronics 11JNO05.*
35. RAJAEI, E. & BORJI, M. A. 2015b. Substrate Index Dependence of Energy Levels in In_(0.4) Ga_(0.6) As/GaAs Quantum Dots Applicable to QD-Lasers (a six-band k.p approximation). *arXiv:1511.00997 [physics.comp-ph] (unpublished observations).*
36. ROSSETTI, M., FIORE, A., SĘK, G., ZINONI, C. & LI, L. 2009. Modeling the temperature characteristics of InAs/GaAs quantum dot lasers. *Journal of Applied Physics,* 106**,** 023105.
37. SCHMIDT, G. Y. A. A. N. M. 1999. Handbook Series on Semiconductor Parameters. *World Scientific, London,* vol. 2**,** 62-88.
38. SHAFIEENEZHAD, A., RAJAEI, E. & YAZDANI, S. 2014. The Effect of Inhomogeneous Broadening on Characteristics of Three-State Lasing InGaAs/GaAs Quantum Dot Lasers. *International Journal of Scientific Engineering and Technology,* 3**,** 297- 301.
39. SHAHRAKI, M. & ESMAILI, E. 2012. Computer simulation of quantum dot formation during heteroepitaxial growth of thin films. *Journal of Theoretical and Applied Physics,* 6**,** 1-5.
40. SHI, Z., HUANG, L., YU, Y., TIAN, P. & WANG, H. 2011. Influence of V/III ratio on QD size distribution. *Frontiers of Optoelectronics in China,* 4**,** 364-368.
41. SINGH, J. 1993. *Physics of Semiconductors and Their Heterostructures*, McGraw-Hill.
42. T.P.PEARSALL 1982. GaInAsP Alloy Semiconductors. *John Wiley and Sons.*
43. TRELLAKIS, A., ZIBOLD, T., ANDLAUER, T., BIRNER, S., SMITH, R. K., MORSCHL, R. & VOGL, P. 2006. The 3D nanometer device project nextnano: Concepts, methods, results. *Journal of Computational Electronics,* 5**,** 285-289.
44. VAFAFARD, A., GOHARSHENASAN, S., NOZARI, N., MORTEZAPOUR, A. & MAHMOUDI, M. 2013. Phase-dependent optical bistability in the quantum dot nanostructure molecules via inter-dot tunneling. *Journal of Luminescence,* 134**,** 900-905.
45. WOOLLEY, J. C., THOMAS, M. B. & THOMPSON, A. G. 1968. Optical energy gap variation in GaxIn1−x As alloys. *Canadian Journal of Physics,* 46**,** 157-159.
46. YEKTA KIYA, Y., RAJAEI, E. & FALI, A. 2012. Study of response function of excited and ground state lasing in InGaAs/GaAs quantum dot laser. *J. Theor. Phys. ,* 1**,** 246-256.
47. YU, C. 2010. Fundamentals of Semiconductors. *Springer.*
48. ZHAO, C., CHEN, Y. H., CUI, C. X., XU, B., SUN, J., LEI, W., LU, L. K. & WANG, Z. G. 2005. Quantum-dot growth simulation on periodic stress of substrate. *The Journal of Chemical Physics,* 123**,** -.